JOURNAL OF MECHANICS OF CONTINUA AND MATHEMATICAL SCIENCES
www.journalimcms.org

ISSN (Online) : 2454 -7190 Vol.-15, No.-3, March (2020) pp 1-18 ISSN (Print) 0973-8975

STEADY FLOW OF AN OLDROYD-B FLUID THROUGH A FOUR-TO-ONE ABRUPT CONTRACTION

Khalifa Mohammad Helal

Department of Mathematics, Comilla University, Cumilla, Bangladesh

Corresponding Author: Khalifa Mohammad Helal

Email: khalifahelal@gmail.com

https://doi.org/10.26782/jmcms.2020.03.00001

Abstract

This study looks the steady problem which models the behavior of incompressible non-Newtonian viscoelastic Oldroyd-B fluid through a four-to-one abrupt contraction in a bidimensional domain $\Omega \subset R^2$.The constitutive equations for the Oldroyd-B fluids consist of highly non-linear system of partial differential equations (PDE) of combined elliptic-hyperbolic type. The numerical results are obtained by a technique of decoupling the system into the Navier-Stokes like problems for the velocity and pressure (elliptic part of the system) and the steady tensorial transport equation for the extra stress tensor (hyperbolic part of the system). To approximate the velocity and pressure, $\mathbb{p}_1 - \mathbb{p}_2$ (Hood-Taylor) finite elements method is used whilethe discontinuous Galerkin finite element ($\mathbb{p}_1 - dc$) method is used to solve the tensorial transport part to approximate the extra stress tensor. Through the flow over four-to-one abrupt contraction domain, the effects of varying the parameters, i.e., i.e., Reynolds number, Weissenberg number, relaxation and retardation time parameter, on the contours of the velocity profile, stream line, pressure and extra stress tensor are presented, analyzed and discussed graphically.

Keywords: Viscoelastic fluid, Oldroyd-B fluid, Navier-Stokes equations, tensorial transport equations, finite element method, abrupt contraction.

I. Introduction

This work aims to study the analysis (mathematical and numerical) and numerical simulations, using finite element methods (FEM), of the non-linear system of partial differential equations (PDE) of a combined elliptic-hyperbolic type, that models the non-Newtonian incompressible viscoelastic Oldroyd-B fluid flows over a four-to-one abrupt contraction in the steady case in a bi-dimensional domain $\Omega \subset \mathrm{R}^2$. We apply the fixed-point type method proposed by Najib and Sandri .

In recent years, many researchers have shown their much interest in the study of non-Newtonian fluids for their applications in the industry and engineering and biological sectors. In the non-Newtonian fluids, the relationship between the Cauchy stress and strain rate tensor is not linear. The viscoelastic fluids, a particular type of non-Newtonian fluids, have both the viscous (characteristics of fluids) and the elastic (characteristics of solids) properties. It cannot be explained by a single relationship between stress and strain rate tensor. Consequently, there are many models exist to describe the behavior of non-Newtonian viscoelastic fluids. The constitutive equations provide us to characterize the mechanical behavior of fluid which relates the Cauchy stress tensor with the kinematics of different quantities. The constitutive equations for non-Newtonian viscoelastic fluids consists of highly non-linear system of partial differential equations (PDE) of combined elliptic-hyperbolic or parabolic-hyperbolic type, and the complexity of this system provides lack of analytical solutions, which makes the researchers interested in its numerical approximation. The Oldroyd-B fluid model is the constitutive model of rate type which is capable to describe the viscoelastic behavior of flows in the polymeric processing and it can describe both the relaxation and retardation time effects..

In this study, we start with the formulation of the constitutive equations of incompressible non-Newtonian Oldroyd-B fluids flows. Then the differential form of the constitutive equations of incompressible non-Newtonian fluids of Oldroyd-B type is deduced which describes the viscoelastic behavior of the fluid. The Oldroyd-B constitutive equations for steady flow is a combined problem having two auxiliary problems, namely, the Navier-Stokes like problems for the velocity and pressure (elliptic part of the system) and the steady tensorial transport equation for the extra stress tensor (hyperbolic part of the system). Both of the auxiliary problems are studied separately in our previous works. Thiscombined Oldroyd-B model has three unknowns: the velocity components$\mathbf{u}$, the pressure$p$, and the viscoelastic extra stress tensor $\boldsymbol{\sigma}$. We use iterative scheme to solve this system. If $\boldsymbol{\sigma}$ is fixed, the model defines a Navier-Stokes systems in the variables $\mathbf{u}$and$p$, which is analyzed using the Hood-Taylor ($\mathbb{p}_1 - \mathbb{p}_2$) finite element method for the approximation of the velocity and the pressure field $(\mathbf{u}, p)$. On the other hand, if $\mathbf{u}$ (and$p$) are fixed, then the model is transformed into a transport problem in the variable $\boldsymbol{\sigma}$. The approximation of $\boldsymbol{\sigma}$ is done by using discontinuous Galerkin finite element ($\mathbb{p}_1 - dc$) method, as discussed in.

We present the approach and discrete problem of Oldroyd-B model. Based on our previous works, the numerical simulations of Oldroyd-B fluids flows problem are discussed. The numerical results for the four-to-one abrupt contraction in a plane domain are analyzed. The behaviors of the solutions are discussed and are compared for different cases. The maximum limit points of the Weissenberg number are found from the solutions at various high values of the Weissenberg numbers.

All the simulations are straightforwardly implemented with the script developed in finite element solver FreeFem++ .

II. Nomenclature

Before discussing the mathematical analysis of Oldroyd-B fluid flows,we introduce some notations of different function spaces in the following table, details of which can be found in.

$L^p(\Omega)$: The Lebesgue spaces	$H^m(\Omega)$: $W^{m,p}(\Omega)$, for $p=2$
$W^{m,p}(\Omega)$, : The standard Sobolev spaces where $m \geq 0$ be an integer and $1 \leq p \leq \infty$	$L^p(\Omega)$: $W^{0,p}(\Omega)$
$\|\cdot\|_{m,p}$: Norms of $W^{m,p}(\Omega)$	$C(\Omega)$: Vector space continuous functions
Re: Reynolds number	We: Weissenberg number

III. The Constitutive Law and Problem Formulation for Oldroyd-B Model

The constitutive relations provide us to characterize the mechanical behavior of fluid. For simple, isotropic, incompressible fluid, the Cauchy stress tensor **T** can be expressed as

$$\mathbf{T} = -p\mathbf{I} + \boldsymbol{\tau}_s$$

where$p$is the hydrostatic pressure, $\boldsymbol{\tau}_s$ is the extra stress tensor and **I** is the identity matrix.

Non-Newtonian Fluids

If for a fluid, the dissipative effects of frictional forces can be described by a linear relation between the extra stress tensor and rate of strain tensor, i.e.,

$$\tau_s = 2\mu\mathbf{D}(\mathbf{u})(\text{Stokes law}) \tag{1}$$

then this fluid is called Newtonian fluid. In (1), $\mu > 0$ is the dynamic viscosity coefficient expressing the fluid's resistance which it offers to shear strain during the displacement $([\mu] = Pa\ s)$, $\mathbf{D}(\mathbf{u}) = \frac{1}{2}[\nabla\mathbf{u} + (\nabla\mathbf{u})^t]$ is the symmetric part of the velocity gradient. On the other hand, the fluids for which the relation between the Cauchy stress tensor and the strain rate tensor is non-linear (doesn't obey the Stokes law) are called non-Newtonian fluids.

Models of Viscoelastic Fluids of Oldroyd Type

Oldroyd observed that the convected time derivative $\frac{D\boldsymbol{\pi}}{Dt} = \frac{\partial\boldsymbol{\pi}}{\partial t} + (\mathbf{u}.\nabla)\boldsymbol{\pi}$ of a tensor $\boldsymbol{\pi}$ is not objective. The objective form of the time derivative of a tensor can be expressed as

$$\frac{D_a\boldsymbol{\pi}}{Dt} = \frac{\partial\boldsymbol{\pi}}{\partial t} + (\mathbf{u}.\nabla)\boldsymbol{\pi} + \boldsymbol{\pi}\mathbf{W}(\mathbf{u}) - \mathbf{W}(\mathbf{u})\boldsymbol{\pi} - a[\boldsymbol{\pi}\mathbf{D}(\mathbf{u}) + \mathbf{D}(\mathbf{u})\boldsymbol{\pi}] \tag{2}$$

where $-1 \leq a \leq 1$ is a parameter, $\mathbf{W}(\mathbf{u}) = \frac{1}{2}[\nabla\mathbf{u} - (\nabla\mathbf{u})^t]$ is the rate of vorticity tensor.

The case with $a = -1$, $a = 1$ and $a = 0$ are respectively called lower, upper and co-rotational convected time derivative.

Oldroyd suggested a general form of constitutive equation as

$$\lambda_1 \frac{D_a \boldsymbol{\tau}_s}{Dt} + \boldsymbol{\tau}_s + \gamma(\boldsymbol{\tau}_s, \nabla\mathbf{u}) = 2\mu\left[\lambda_2 \frac{D_a \mathbf{D}(\mathbf{u})}{Dt} + \mathbf{D}(\mathbf{u})\right], \qquad 0 \leq \lambda_2 < \lambda_1 \tag{3}$$

where the tensor $\boldsymbol{\tau}_s$ is the extra stress, $\lambda_1 \geq 0$ and $\lambda_2 \geq 0$ are the constants depend on the continuous medium, respectively, called the relaxation and retardation time of fluid, $\gamma(\boldsymbol{\tau}_s, \nabla\mathbf{u})$is a tensor defined by the traces of $\boldsymbol{\tau}_s$ and /or $\mathbf{D}(\mathbf{u})$. There are several types of general models with$\gamma(\boldsymbol{\tau}_s, \nabla\mathbf{u}) = 0$, e.g.,

- Maxwell type fluid models ($\lambda_2 = 0$).
- Jeffreys type fluid models ($\lambda_2 \neq 0$).
- Oldroyd-A fluid ($\lambda_1 > \lambda_2 > 0$ and $a = -1$).
- Oldroyd-B fluid ($\lambda_1 > \lambda_2 > 0$ and $a = 1$).

Models of the Fluids of Oldroyd-B Type

Letλ_1 and λ_2 are the measures of the time for which the fluid remembers the flow history. Decomposing the extra-stress tensor $\boldsymbol{\tau}_s$ into the sum of its Newtonian part $\boldsymbol{\sigma}_n$ and its viscoelastic part $\boldsymbol{\sigma}_e$, we can write $\boldsymbol{\tau}_s = \boldsymbol{\sigma}_n + \boldsymbol{\sigma}_e$

where $\boldsymbol{\sigma}_n = 2\mu\frac{\lambda_2}{\lambda_1}\mathbf{D}(\mathbf{u})$, with $\mu_n = \mu\frac{\lambda_2}{\lambda_1}$the coefficient of Newtonian viscosity.

Therefore, the Cauchy stress tensor can be written as

$$\mathbf{T} = -p\mathbf{I} + \boldsymbol{\sigma}_n + \boldsymbol{\sigma}_e = -p\mathbf{I} + 2\mu\frac{\lambda_2}{\lambda_1}\mathbf{D}(\mathbf{u}) + \boldsymbol{\sigma}_e (4)$$

From (3), for Oldroyd-B fluid, i.e., for $\gamma(\tau_s, \nabla\boldsymbol{u}) = 0$, $\lambda_1 > \lambda_2 > 0$ and $a = 1$, the general form of the constitutive equation can be written as

$$\lambda_1 \frac{D_a \boldsymbol{\sigma}_e}{Dt} + \boldsymbol{\sigma}_e = 2\mu_e \mathbf{D}(\mathbf{u}) \tag{5}$$

where$\mu_e = \mu - \mu_n$ is the coefficient of elastic viscosity and $\mu = \mu_e + \mu_n$.

Finally, we can write by (2)

$$\lambda_1\left[\frac{\partial\boldsymbol{\sigma}_e}{\partial t} + (\mathbf{u}.\nabla)\boldsymbol{\sigma}_e\right] + \boldsymbol{\sigma}_e = 2\mu_e\mathbf{D}(\mathbf{u}) - \lambda_1[\boldsymbol{\sigma}_e\mathbf{W}(\mathbf{u}) - \mathbf{W}(\mathbf{u})\boldsymbol{\sigma}_e - \boldsymbol{\sigma}_e\mathbf{D}(\mathbf{u}) - \mathbf{D}(\mathbf{u})\boldsymbol{\sigma}_e] \tag{6}$$

Taking into account (2.24), the conservation law of momentum can be written as follows

$$\rho\frac{\partial\mathbf{u}}{\partial t} + \rho(\mathbf{u}.\nabla)\boldsymbol{u} = -\nabla p + 2\mu_n\nabla.\mathbf{D}(\mathbf{u}) + \nabla.\boldsymbol{\sigma}_e + \rho\mathbf{f} \tag{7}$$

If $\nabla.\mathbf{u} = 0$, the conservation of momentum can be written as

$$\rho\frac{\partial \mathbf{u}}{\partial t}+\rho(\mathbf{u}.\nabla)\mathbf{u}=-\nabla p+\mu_n\,\Delta\mathbf{u}+\nabla.\boldsymbol{\sigma}_e+\rho\mathbf{f}$$

For the simplicity, we write $\boldsymbol{\sigma}$ instead of $\boldsymbol{\sigma}_e$. Oldroyd-B model can be described by the non-linear equations formed by the law of conservation of mass, the momentum equations and the form of transport equations, which can be written in the domain Ω as ,

$$\begin{cases}\rho\frac{\partial \mathbf{u}}{\partial t}+\rho(\mathbf{u}.\nabla)\mathbf{u}-\mu_n\,\Delta\mathbf{u}+\nabla p=\nabla.\boldsymbol{\sigma}+\rho\,\mathbf{f}\text{ in }\Omega,\\ \nabla.\mathbf{u}=0\text{ in }\Omega,\\ \lambda_1\left[\frac{\partial\boldsymbol{\sigma}}{\partial t}+(\mathbf{u}.\nabla)\boldsymbol{\sigma}\right]+\boldsymbol{\sigma}=2\mu_e\mathbf{D}(\mathbf{u})-\lambda_1[\boldsymbol{\sigma}\mathbf{W}(\mathbf{u})-\mathbf{W}(\mathbf{u})\boldsymbol{\sigma}-\boldsymbol{\sigma}\mathbf{D}(\mathbf{u})-\mathbf{D}(\mathbf{u})\boldsymbol{\sigma}]\text{in }\Omega.\end{cases}\qquad(8)$$

Assuming $\mathbf{h}(\boldsymbol{\sigma},\nabla\mathbf{u})=2\mu_e\mathbf{D}(\mathbf{u})-\lambda_1[\boldsymbol{\sigma}\mathbf{W}(\mathbf{u})-\mathbf{W}(\mathbf{u})\boldsymbol{\sigma}-\boldsymbol{\sigma}\mathbf{D}(\mathbf{u})-\mathbf{D}(\mathbf{u})\boldsymbol{\sigma}]$

$=2\mu_e\mathbf{D}(\mathbf{u})+\lambda_1[(\nabla\mathbf{u})\boldsymbol{\sigma}+\boldsymbol{\sigma}(\nabla\mathbf{u})^{\mathrm{t}}]$,

equations (8) can be written as

$$\begin{cases}\rho\frac{\partial \mathbf{u}}{\partial t}+\rho(\mathbf{u}.\nabla)\mathbf{u}-\mu_n\,\Delta\mathbf{u}+\nabla p=\nabla.\boldsymbol{\sigma}+\rho\,\mathbf{f}\text{ in }\Omega,\\ \nabla.\mathbf{u}=0\text{ in }\Omega,\\ \lambda_1\left[\frac{\partial\boldsymbol{\sigma}}{\partial t}+(\mathbf{u}.\nabla)\boldsymbol{\sigma}\right]+\boldsymbol{\sigma}=\mathbf{h}(\boldsymbol{\sigma},\nabla\mathbf{u}),\quad\text{in }\Omega.\end{cases}\qquad(9)$$

We observe that the conservation of momentum leads the symmetry properties of the tensor $\boldsymbol{\sigma}$, i.e., $\boldsymbol{\sigma}^t=\boldsymbol{\sigma}$.

The problem (9) is a mixed problem. The first two equations form a parabolic system for $(\mathbf{u},p)$which is in the form of Navier-stokes equation. The last equation has a hyperbolic characteristic which is in the form of Transport equation.

In case of steady flow, the Oldroyd-B constituive equations can be written as

$$\begin{cases}\rho(\mathbf{u}.\nabla)\mathbf{u}-\mu_n\,\Delta\mathbf{u}+\nabla p=\nabla.\boldsymbol{\sigma}+\rho\mathbf{f}\text{ in }\Omega,\\ \nabla.\mathbf{u}=0\text{ in }\Omega,\\ \lambda_1(\mathbf{u}.\nabla)\boldsymbol{\sigma}+\boldsymbol{\sigma}=\mathbf{h}(\boldsymbol{\sigma},\nabla\mathbf{u})\text{in }\Omega.\end{cases}\qquad(10)$$

Let L be the characteristic length, U represents a characteristic velocity of the flow and $\mu=\mu_e+\mu_n$ be the viscosity coefficient, Re be the Reynolds number, and We be Weissenbergnumber. To obtain a system of dimensionless variables**,** let us use the following transformations:

$$\mathbf{x}=\frac{\mathbf{x}'}{L},\quad t=\frac{t'}{T}=\frac{Ut'}{L},\quad \mathbf{u}=\frac{\mathbf{u}'}{U},\quad \boldsymbol{\sigma}=\frac{\boldsymbol{\sigma}'L}{\mu\,U},\quad p=\frac{p'L}{\mu\,U}\quad \mathbf{f}=\frac{\mathbf{f}'L^2}{\mu\,U}$$

$$Re=\rho\frac{UL}{\mu}=\frac{UL}{\nu},We=\lambda_1\frac{U}{L}$$

where the symbol $'$ is attached to dimensional parameters.

The dimensionless form of the system (8) can be written as

$$\begin{cases}Re[\frac{\partial\mathbf{u}}{\partial t}+(\mathbf{u}\cdot\nabla)\mathbf{u}]+\nabla p=(1-\lambda)\,\Delta\mathbf{u}+\nabla.\boldsymbol{\sigma}+\mathbf{f},\text{in }\Omega,\\ \nabla\cdot\mathbf{u}=0,\text{in}\Omega,\\ We\frac{D_a\boldsymbol{\sigma}}{Dt}+\boldsymbol{\sigma}=2\lambda\,\mathbf{D}(\mathbf{u}),\ \text{in}\Omega.\end{cases}\qquad(11)$$

where $\lambda = 1 - \frac{\lambda_2}{\lambda_1} = \frac{\mu_e}{\mu_e+\mu_n}$, is the retardation parameter $(0 < \lambda < 1)$, and $\lambda_2 \geq 0$ is the retardation time of fluid.

In case of stationary motion, the problem can be written as

find$(\mathbf{u}, p, \boldsymbol{\sigma})$ defined in Ω such that,

$$\begin{cases} Re[(\mathbf{u}.\nabla)\mathbf{u}] + \nabla p = (1-\lambda)\Delta\mathbf{u} + \nabla.\boldsymbol{\sigma} + \mathbf{f} \text{ in } \Omega, \\ \nabla.\mathbf{u} = 0 \text{ in } \Omega, \\ We[(\mathbf{u}.\nabla)\boldsymbol{\sigma}] + \boldsymbol{\sigma} = 2\lambda\,\mathbf{D}(\mathbf{u}) + We[(\nabla\mathbf{u})\boldsymbol{\sigma} + \boldsymbol{\sigma}(\nabla\mathbf{u})^{t}] \text{in } \Omega. \end{cases} \tag{12}$$

The above equation is composed of a Navier-Stokes like system for $(\mathbf{u}, p)$ and a transport equation for extra stress tensor $\boldsymbol{\sigma}$.

Finally, the system (10) should be completed with a set of initial and boundary conditions, which depend on the considered geometry. In our case, we consider four-to-one abrupt contraction. Taking $\Omega \subset \mathrm{R}^2$ a bounded, simply connected domain, the boundary conditions ensuring feasibility of numerical solution are:

(i) Dirichlet boundary conditions for the velocity on the boundary $\partial\Omega$

$$\mathbf{u} = \mathbf{g} \text{ on } \partial\Omega$$

with compatibility condition

$$\int_{\partial\Omega} \mathbf{g}.\mathbf{n} = 0,$$

where$\mathbf{n}$ is the unit outward normal vector to Ωat the boundary $\partial\Omega$. For homogeneous case, $\mathbf{g} = 0$.

(ii) For the stress, a condition on the upstream boundary section

$$\partial\Omega^- = \{\mathbf{x} \in \partial\Omega : \mathbf{u}(\mathbf{x}).\mathbf{n}(\mathbf{x}) < 0\}$$
$$\boldsymbol{\sigma} = \boldsymbol{\sigma}_{\partial\Omega} \text{on} \partial\Omega^-.$$

With the homogeneous Dirichlet boundary conditions, the Oldroyd-B fluid model problem is well-posed.

With the homogeneous Dirichlet boundary conditions defined over Ω, the Oldroyd-B problem can be reformulated as follows:

find the quantities $\boldsymbol{\sigma}$, $\mathbf{u}$ and p defined in Ω such that

$$\begin{cases} \rho(\mathbf{u}.\nabla)\mathbf{u} - \mu_n \Delta\mathbf{u} + \nabla p = \nabla.\boldsymbol{\sigma} + \rho\,\mathbf{f}, \text{in } \Omega, \\ \nabla.\mathbf{u} = 0, \text{in } \Omega, \\ \lambda_1(\mathbf{u}.\nabla)\boldsymbol{\sigma} + \boldsymbol{\sigma} = \mathbf{h}(\boldsymbol{\sigma}, \nabla\mathbf{u}), \text{in } \Omega, \\ \mathbf{u} = 0, \text{on} \partial\Omega \end{cases} \tag{13}$$

subject to the boundary condition (ii).

For non-dimensional case, the problem (13) can be read as the form of (12) as follows:

Find the non-dimensional quantities,denoted by $\boldsymbol{\sigma}$, $\mathbf{u}$ and p, defined in Ω such that,

$$\begin{cases} Re[(\mathbf{u}.\nabla)\mathbf{u}] + \nabla p = (1-\lambda)\Delta\mathbf{u} + \nabla.\boldsymbol{\sigma} + \mathbf{f}, \text{in } \Omega, \\ \nabla.\mathbf{u} = 0 \text{ in } \Omega, \\ We[(\mathbf{u}.\nabla)\boldsymbol{\sigma}] + \boldsymbol{\sigma} = 2\lambda\,\mathbf{D}(\mathbf{u}) + We[(\nabla\mathbf{u})\boldsymbol{\sigma} + \boldsymbol{\sigma}(\nabla\mathbf{u})^{t}], \text{in } \Omega. \end{cases} \tag{14}$$

subject to the boundary conditions in (i) and (ii).

Variational Formulation

In this work, we consider the fluid confined into a rectangular domain Ω with fixed boundary $\partial\Omega$. Mathematically, we write the steady Oldroyd-B equations with the Dirichlet boundary conditions, i.e., $\mathbf{u} = \mathbf{u}_0$such that $\mathbf{u}_0.\mathbf{n} = 0$ on$\partial\Omega$. So, given an external force field $\mathbf{f} \in \mathbf{H}^{-1}(\Omega)$ and $0 < \lambda < 1$ the viscoelastic fraction of the viscosity, the steady Oldroyd-B problem is defined by,

$$\begin{cases} Re[(\mathbf{u}.\nabla)\mathbf{u}] + \nabla p = (1-\lambda)\Delta\mathbf{u} + \nabla.\boldsymbol{\sigma} + \mathbf{f}, \text{ in } \Omega, \\ \nabla.\mathbf{u} = 0, \text{in } \Omega, \\ We[(\mathbf{u}.\nabla)\boldsymbol{\sigma}] + \boldsymbol{\sigma} = 2\lambda\, \mathbf{D}(\mathbf{u}) + We[(\nabla\mathbf{u})\boldsymbol{\sigma} + \boldsymbol{\sigma}(\nabla\mathbf{u})^t], \text{ in } \Omega \\ \mathbf{u} = \mathbf{u}_0, \mathbf{u}_0.\mathbf{n} = 0, \text{ on} \partial\Omega \end{cases} \tag{15}$$

Considering $\mathbf{v} \in \mathbf{H}_0^1(\Omega)$, $q \in L_0^2(\Omega)$, and $\boldsymbol{\tau} \in \mathbf{L}_s^2(\Omega)$ as arbitrary test functions, and taking the scalar product between the momentum equation and $\mathbf{v}$, between the transport equation and $\boldsymbol{\tau}$, and multiplying the continuity equation by q and finally integrating all of them over Ω, we obtain the variational form to Oldroyd-B problem as,

Given$\mathbf{f} \in \mathbf{H}^{-1}(\Omega)$, find $(\mathbf{u}, p, \boldsymbol{\sigma}) \in \mathbf{H}_0^1(\Omega) \times L_0^2(\Omega) \times \mathbf{L}_s^2(\Omega)$ such that

$$\begin{cases} \int_\Omega Re[(\mathbf{u}.\nabla)\mathbf{u}.\mathbf{v}] + \int_\Omega (1-\lambda)\nabla\mathbf{u}:\nabla\mathbf{v} + \int_\Omega \sigma:\nabla\mathbf{v} - \int_\Omega p\nabla\cdot\mathbf{v} = +\int_\Omega \mathbf{f}.\mathbf{v} \\ \int_\Omega q\nabla.\mathbf{u} = 0 \\ \int_\Omega \boldsymbol{\sigma}:\boldsymbol{\tau} + \int_\Omega We[(\mathbf{u}.\nabla)\boldsymbol{\sigma}]:\boldsymbol{\tau} - \int_\Omega We[(\nabla\mathbf{u})\boldsymbol{\sigma} + \boldsymbol{\sigma}(\nabla\mathbf{u})^t]:\tau = \int_\Omega 2\lambda\, \mathbf{D}(\mathbf{u}):\boldsymbol{\tau} \end{cases} \tag{16}$$

for all $(\mathbf{v}, p, \boldsymbol{\tau}) \in \mathbf{H}_0^1(\Omega) \times L_0^2(\Omega) \times \mathbf{L}_s^2(\Omega)$

Finite Element Approximation of Oldroyd-B Problem

In this section, we study the approximation of the problem (13) using finite element method. The system (13) is a composed problem for the three unknowns $(\mathbf{u}, p, \boldsymbol{\sigma})$. If $\boldsymbol{\sigma}$ is fixed, the first two equations of (13) defines a Navier-Stokes system in the variables $\mathbf{u}$and$p$. As in, we use the Hood-Taylor finite element method for the approximation of the velocity and the pressure field $(\mathbf{u}, p)$. If $\mathbf{u}$ (and$p$) are fixed, then the third equation of (13) is a transport equation in the variable $\boldsymbol{\sigma}$. The approximation of $\boldsymbol{\sigma}$ will be done by using discontinuous Galerkin finite element method, as in.

Consider the case where $0 < \lambda < 1$.

Let $\mathcal{T}_h, h > 0$, where $, h$ is discretization parameter, be a non-degenerated regular triangulation of Ω such that $\overline{\Omega} = \bigcup_{K\in\mathcal{T}_h} K$.

Let $\mathbf{V}_h$ and Q_h be two finite-dimensional spaces for the velocity and the pressure, respectively, such that $\mathbf{V}_h \in \mathbf{H}^1(\Omega)$ and $Q_h \in L_0^2(\Omega)$. We define the pair of discrete space $\mathbf{V}_h^0 = \mathbf{V}_h \cap \mathbf{H}_0^1(\Omega)$ and $M_h = Q_h \cap L_0^2(\Omega)$ which correspond to Hood-Taylor finite element method. We also consider the space

$\mathbf{T}_h = \{\sigma_h \in \mathbf{T} \cap \mathbf{C}(\Omega) | \boldsymbol{\sigma}_{h|K} \in \mathbb{P}_1, \forall K \in \mathcal{T}_h \subset \mathrm{S}_1^{\mathrm{d}\times\mathrm{d}}$,

$$T = \{\boldsymbol{\sigma} \in L^2(\Omega) | \mathbf{u}\cdot\nabla\boldsymbol{\sigma} \in L^2(\Omega), \sigma_{12} = \sigma_{21}\}.$$

The Oldroyd-B model is approached by the following problem:

Given$\mathbf{f} \in \mathbf{H}^{-1}(\Omega)$, find $(\mathbf{u}_\mathrm{h}, p_h, \sigma_h) \in \mathbf{V}_h^0 \times M_h \times \mathbf{T}_h$ such that

$$\begin{cases} a(\mathbf{u}_h, \mathbf{v}_h) + c(\mathbf{u}_h, \mathbf{u}_h, \mathbf{v}_h) + b(\mathbf{v}_h, p_h) = (\nabla . \boldsymbol{\sigma}_h + \mathbf{f}, \mathbf{v}_h), \forall \mathbf{v}_h \in \mathbf{V}_h^0 \\ b(\mathbf{u}_h, q_h) = 0, \forall q_h \in M_h, \\ (\boldsymbol{\sigma}_h, \boldsymbol{\tau}_h) + (\mathbf{u}_h \cdot \nabla . \boldsymbol{\sigma}_h, \boldsymbol{\tau}_h) + (\phi^*_{\partial K}(\boldsymbol{\sigma}_h), \boldsymbol{\tau}_h) = (\mathbf{h}(\nabla \mathbf{u}, \boldsymbol{\sigma}), \boldsymbol{\tau}_h), \quad \forall \boldsymbol{\tau}_h \in \mathbf{W} \end{cases} \tag{17}$$

with the interface and boundary adjoint-fluxes

$$\phi^{*,i}(\boldsymbol{\sigma}_h)|\partial K = \left(\alpha|\mathbf{u} \cdot \mathbf{n}_\mathrm{k}| - \frac{1}{2}\mathbf{u} \cdot \mathbf{n}_\mathrm{k}\right)[[\boldsymbol{\sigma}_h]]\partial K, \tag{18}$$

$$\phi^{*,\partial}(\boldsymbol{\sigma}_h)|\partial K = -|\mathbf{u} \cdot \mathbf{n}|\boldsymbol{\sigma}_h \chi_{\partial\Omega^-} \tag{19}$$

where$\alpha > 0$ is a parameter and $\chi_{\partial\Omega^-}$denotes the characteristic function of $\partial\Omega^-$.

The nondimensional approach problem can be written as follows:

Given$\mathbf{f} \in \mathbf{H}^{-1}(\Omega)$, find $(\mathbf{u}_\mathrm{h}, p_h, \sigma_h) \in \mathbf{V}_h^0 \times M_h \times \mathbf{T}_h$ such that

$$\begin{cases} \int_\Omega Re[(\mathbf{u}_h . \nabla)\mathbf{u}_h . \mathbf{v}_h] + \int_\Omega (1-\lambda)\nabla \mathbf{u}_h : \nabla \mathbf{v}_h + \int_\Omega \sigma_h : \nabla \mathbf{v}_h - \int_\Omega p_h \nabla . \mathbf{v}_h = \int_\Omega \mathbf{f} . \mathbf{v}_h \\ \int_\Omega q_h \nabla . \mathbf{u}_h = 0, \\ \int_\Omega \sigma_h : \tau_h + \int_\Omega We[(\mathbf{u}_h . \nabla)\sigma_h] : \tau_h - \int_\Omega We[(\nabla \mathbf{u}_h)\sigma_h + \sigma_h(\nabla \mathbf{u}_h)^t] : \tau_h + (\phi^*_{\partial K}(\boldsymbol{\sigma}_h), \boldsymbol{\tau}_h) = \int_\Omega 2\lambda\, \mathbf{D}(\mathbf{u}_h) : \tau_h, \end{cases} \tag{20}$$

$\forall \mathbf{v}_h \in \mathbf{V}_h^0, \forall q_h \in M_h, \forall \tau_h \in \mathbf{T}_h$.

Algorithm to Approximate the Oldroyd-B Problem

The extra-stress tensor is computed separately from the kinematic equations. From a fixed value for the velocity (and pressure) the extra-stress tensor is evaluated. Then the velocity field and pressure are updated with the current extra-stress tensor whose components are treated as known body forces. Repeat the procedure.

- Given $(\mathbf{u}_h^n, p_h^n, \boldsymbol{\sigma}_h^n)$ the approach solution of iteration n, find $(\mathbf{u}_h^{n+1}, p_h^{n+1})$, the solution of
$$\int_\Omega Re[(\mathbf{u}_h^{n+1} . \nabla)\mathbf{u}_h^{n+1} . \mathbf{v}_h] + \int_\Omega (1-\lambda)\nabla \mathbf{u}_h^{n+1} : \nabla \mathbf{v}_h - \int_\Omega p_h^{n+1} \nabla . \mathbf{v}_h = \int_\Omega \boldsymbol{\sigma}_h^n : \nabla \mathbf{v}_h + \int_\Omega \mathbf{f} . \mathbf{v}_h$$
- Given $\mathbf{u}_h^{n+1}$ and $\boldsymbol{\sigma}_h^n$=$\boldsymbol{\sigma}_h^{n_0}$, find the solution $\boldsymbol{\sigma}^*$=$\boldsymbol{\sigma}_h^{n_{k+1}}$ of

$$\int_\Omega \boldsymbol{\sigma}_h^{n_{k+1}} : \tau_h + We\int_\Omega [(\mathbf{u}_h^{n+1} . \nabla)\boldsymbol{\sigma}_h^{n_{k+1}}] : \tau_h + (\phi^*_{\partial K}(\boldsymbol{\sigma}_h^{n_{k+1}}), \tau_h)$$
$$= \int_\Omega We[\boldsymbol{\sigma}_h^{n_k}(\nabla \mathbf{u}_h^{k+1}) + \nabla \mathbf{u}_h^{k+1}\boldsymbol{\sigma}_h^{n_k}] : \tau_h + \int_\Omega 2\lambda\, \mathbf{D}(\mathbf{u}_h^{k+1}) : \tau_h, k \geq 0$$

IV. Numerical Results and Discussions for a Four-to-One Abrupt Contraction

By the implementation of the finite element method in our own script in FreeFem++, we obtain the numerical solutions of theOldroyd-B problem. Here, we consider that the fluid flows in an abrupt contraction (or 4:1 planar contraction) subject to suitable boundary conditions. This type of flow is interesting theoretically and practically, and has been studied by many authors, since 1988. These problems have a lot of applications in polymer processing, especially in extrusion and injection moulding.

We consider that the fluid is confined into a domain Ω with its boundary $\partial\Omega = \bigcup_{k=1}^{8} \partial\Omega_{\mathrm{k}}$ which is shown in Fig. 1.

This domain Ω consists of six boundaries as rigid wall denoted by $\partial\Omega_{\mathrm{w}} = \bigcup \partial\Omega_k$, with

$k = 1, 2, 3, 5, 6, 7$,an inlet or inflow boundary at upstream section $\partial\Omega_8 = S_1$, and an outlet or outflow boundary at downstream section $\partial\Omega_4 = S_2$. The fluid enters into the domain through the upstream section S_1. We consider an inflow parabolic profile at the upstream section for the velocity field and homogeneous no-slip conditions on the wall. To obtain the Poiseuille velocity profiles before the contraction and at downstream, the computational domain Ω is assumed to be long enough at upstream and downstream sections. In our referential domain, we consider the length of upstream section is $5r_1 = 2$, with r_1 the radius of upstream, while the length of downstream section is taken as $10r_1 = 4$. The respective widths of upstream and downstream sections are $2r_1 = 0.8$and $2r_2 = 0.2$.

Taking into account the boundary conditions of Saramito, we impose the boundary conditions, for the problem, which is adapted to our computational domainΩ.

We impose the following boundary conditions:

- Inflow boundary conditions for the velocity and the stresses at the upstream section, i.e., on $\partial\Omega_8 = S_1$:

$$u_1 = \frac{r_2}{8r_1^2}\, y(2r_1 - y) = 0.078125\, y\ (0.8 - y),$$

$$u_2 = 0,$$

$$\sigma_{11} = 2\lambda\, We \left(\frac{\partial u_1}{\partial y}\right)^2,$$

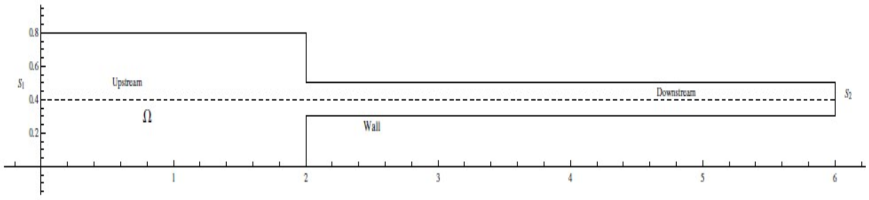

Fig. 1: Computational domain Ω for a 4:1 abrupt contraction.

$$\sigma_{12} = \lambda\, \frac{\partial u_1}{\partial y},$$

$$\sigma_{22} = 0,$$

- Outflow boundary conditions at downstream section, i.e., on $\partial\Omega_4 = S_2$:

$$u_1 = 0$$

$$u_2 = 0$$

- The boundary conditions for the velocity at the wall, i.e., on $\partial\Omega_{\mathrm{w}}$:

$$u_2 = 0$$

So, the Oldroyd-B model problem to compute the flow in an abrupt contraction can be written as

$$\begin{cases} Re[(\mathbf{u}.\nabla)\mathbf{u}] - (1-\lambda)\Delta\mathbf{u} + \nabla p = \nabla.\boldsymbol{\sigma} + \mathbf{f}, \quad \text{in } \Omega \\ \nabla.\mathbf{u} = 0, \text{in } \Omega, \\ \boldsymbol{\sigma} + We[(\mathbf{u}.\nabla)\boldsymbol{\sigma}] = 2\lambda\,\mathbf{D}(\mathbf{u}) + We[(\nabla\mathbf{u})\boldsymbol{\sigma} + \boldsymbol{\sigma}(\nabla\mathbf{u})^{\mathrm{t}}], \text{in } \Omega \\ u_1 = 0.078125\, y\,(0.8-y), \text{on} \partial\Omega_8 = S_1 \\ u_2 = 0, \text{on} \partial\Omega_4 = S_2 \\ u_1 = 0, u_2 = 0, \text{on} \partial\Omega_w \\ \sigma_{11} = 2\lambda\, We\left(\frac{\partial u_1}{\partial y}\right)^2, \text{on} S_1 \\ \sigma_{12} = \lambda\,\frac{\partial u_1}{\partial y}, \ \text{on} S_1 \\ \sigma_{22} = 0, \text{on} S_1 \end{cases} \quad (21)$$

For the numerical results, we use the exact solution of fully developed Poiseuille flow in straight pipe as the initial condition for the tensor while the solution of the Stokes problem is the initial condition for the velocity.

To obtain the numerical simulations of the flow, we take $\lambda = 0.1$, and we discretize the domain Ω on a mesh with 2066 elements where 4405 $\mathbb{p}_2$nodes for the velocity, 1170 $\mathbb{p}_1$ nodes for the pressure and 6198 $\mathbb{p}_1 dc$ nodes for the tensor are defined (Fig.2).

The flow is laminar at upstream and at downstream sections, where the viscous forces are dominant, as we expect. In the opening of narrower domain, we observe a different behavior, where inertial forces are fallen. For this reason, we decide to present a partial view of variables involved in the problem in a neighborhood of contraction.

Newtonian Flows

The simulations were performed to Newtonian flows. We fix $We = 0$ and take several *Re* between 1 and 500 and compare the results. We observe that the quantitative behavior for the kinematic is almost same (Figs. 3-5), (Figs. 6-8), (Figs. 9-11) with a small increase of maximum values and small decrease of minimum values. The pressure is constant along the y-direction and varies linearly with x. In fact, the behavior of pressure is very similar to the Poiseuille flows. The qualitative behavior can be observed and compared easily through the stream function (Figs. 12-14). We observe the recirculation vortices in the corner. These vortices are shrinking when the Reynolds increase. This is the effect of inertia which makes the fluid speedy to enter the narrow part of the domain (tube), pulling the fluid out of the corner to inside the tube, and thus decreasing the vortices. To prove our description, all tests are performed in 3 different cases with $Re = 1, 100$ and 500, and we present the numerical results.

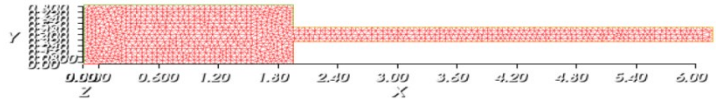

Fig. 2: Mesh with 2066 elements

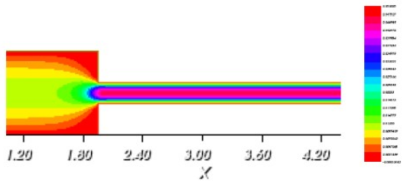

Fig. 3: The first component of the velocity (partial view) with $Re = 1$

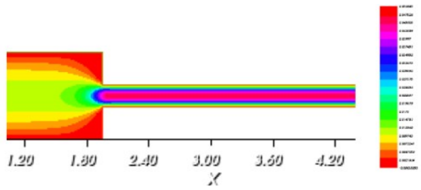

Fig. 4: The first component of the velocity (partial view) with $Re = 100$.

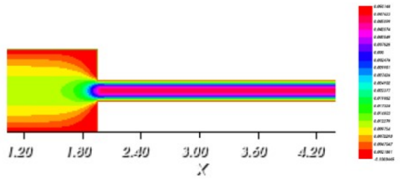

Fig. 5: The first component of the velocity (partial view) with $Re = 500$.

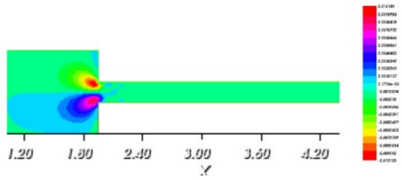

Fig. 6: The second component of the velocity (partial view) with $Re = 1$.

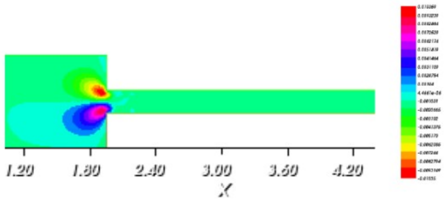

Fig. 7: The second component of the velocity (partial view) with $Re = 100$.

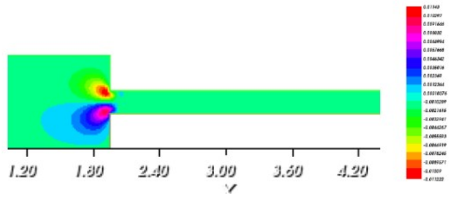

Fig. 8: The second component of the velocity (partial view) with $Re = 500$.

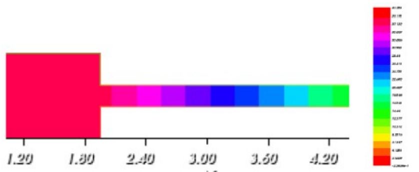

Fig. 9: The pressure (partial view) with $Re = 1$.

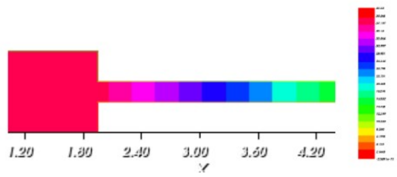

Fig. 10: The pressure (partial view) with $Re = 100$.

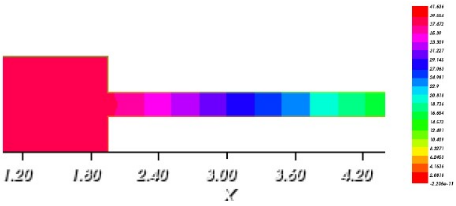

Fig. 11: The pressure (partial view) with $Re = 500$.

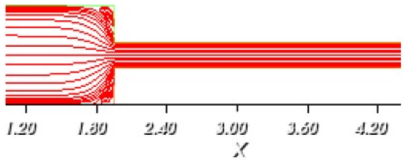

Fig. 12: The stream function (partial view) with $Re = 1$.

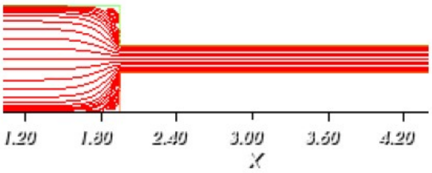

Fig. 13: The stream function (partial view) with $Re = 100$.

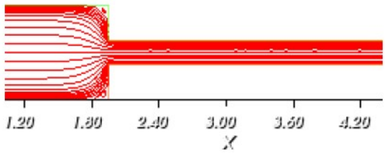

Fig. 14: The stream function (partial view) with $Re = 500$.

Viscoelastic Flows

The simulations were performed to viscoelastic flows. For all performed tests, we observed that the convergence of the algorithm is influenced by the values of Reynolds and Weissenberg, the latter being the main cause for the divergence of the algorithm. In fact, the two re-entrant corners are one of the reasons for which the problem fails to converge if we consider the high value of Weissenberg number. This result may be directly related to the dissipative instability of the model in the elongation flow dominated in the contraction flow near the entrance region.

We test various values of Reynolds to seek the limit of the Weissenberg value, for which the algorithm converges. We observe that when we increase the Re, threshold for We decreases. Table 1 shows the maximum values of Weissenberg numbers We for respective values of Reynold numbers Re, for which the results are convergent.

Table 1: Maximum values of We (We_{max}) for respective values of Re.

Re	1	50	100	250	500
We_{max}	5.13	5.08	5.03	4.86	4.60

For all performed tests, we analyze the behavior of the velocity, pressure and tensor. We observed that the qualitative behaviors of the kinematic are the same for Newtonian flows although we can observe the differences of the types of recirculations, and their zones for the viscoelastic flows in relation to the Newtonian fluids flows through the stream function (compare the Figs.12-14with Figs.15-22). The center of circulating zone moves from the re-entrant corner to the salient edge. We observed the elastic effects. The speeding up along the streamlines in the center causes an elastic tension along these

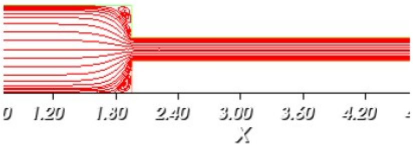

Fig. 15: The stream function (partial view) with $Re = 1$and $We = 1$.

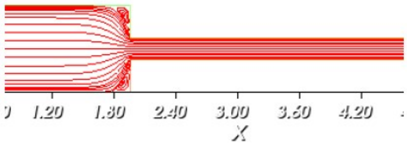

Fig. 16: The stream function (partial view) with $Re = 1$and $We = 4.6$.

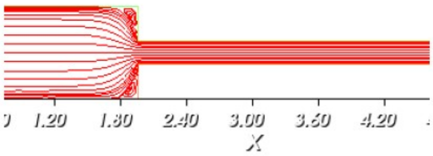

Fig. 17: The stream function (partial view) with $Re = 1$and $We = 5.13$.

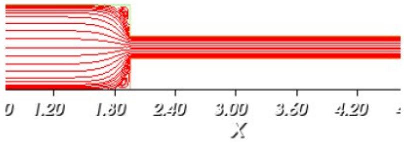

Fig. 18: The stream function (partial view) with

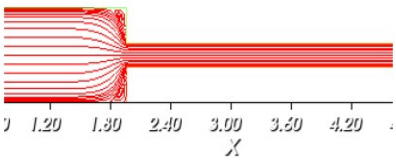

Fig.19: The stream function (partial view) with $Re = 100$and $We = 4.6$.

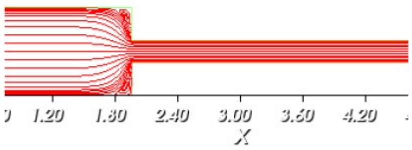

Fig. 20: The stream function (partial view) with $Re = 100$and $We = 5.03$.

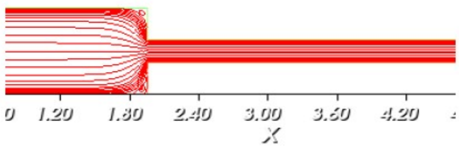

Fig. 21: The stream function with $Re = 500$ and

$We = 1$.

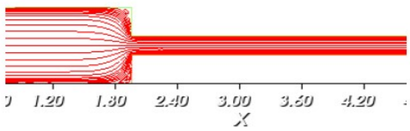

Fig. 22: The stream function with $Re = 500$ and

$We = 4.6$.

streamlines which exerts a pull on the fluid directly upstream and pushes the fluid on the sides back into the corner, and this causes a recirculation zone at which the intensity and the length increase as a combined effect between Re and We parameters.

We observe that the big differences of the behaviors of the components of tensors occur for $\sigma_{11}$and σ_{22}. For theses components, the influence of We is notable. For a fix value of Re, when the We increases, we see the effects as it extend from the corners into the tube and in the case of σ_{22}, also behind the entry of the tube. The next figures (Figs. 23-46) show us the behavior of the components of tensors.

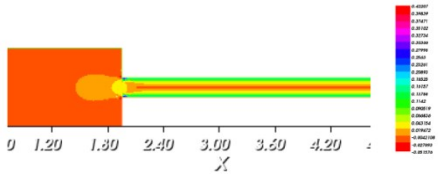

Fig. 23: The component of σ_{11} (partial view) with $Re = 1$and $We = 1$.

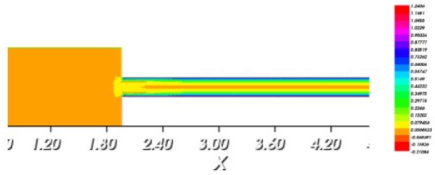

Fig. 24: The component of σ_{11} (partial view) with $Re = 1$and $We = 4.6$.

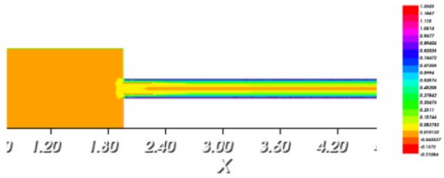

Fig. 25: The component of σ_{11} (partial view) with $Re = 1$and $We = 5.13$.

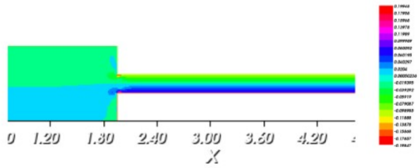

Fig. 26: The component of σ_{12} (partial view) with $Re = 1$and $We = 1$.

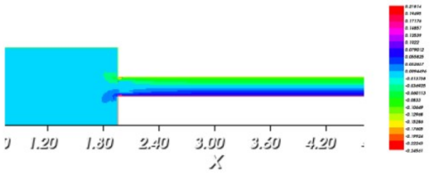

Fig. 27: The component of σ_{12} (partial view) with $Re = 1$and $We = 4.6$.

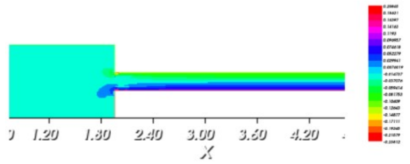

Fig. 28: The component of σ_{12} (partial view) with $Re = 1$and $We = 5.13$.

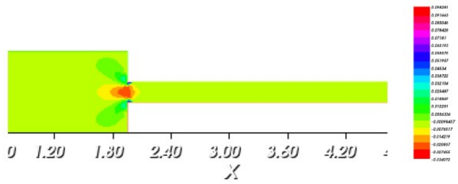

Fig. 29: The component of σ_{22} (partial view) with $Re = 1$and $We = 1$.

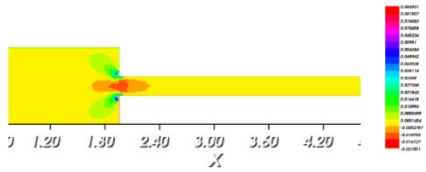

Fig. 30: The component of σ_{22} (partial view) with $Re = 1$and $We = 4.6$.

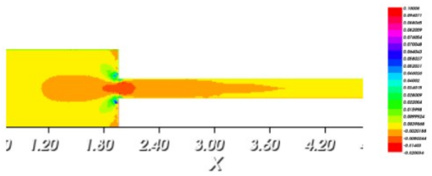

Fig. 31: The component of σ_{22} (partial view) with $Re = 1$and $We = 5.13$.

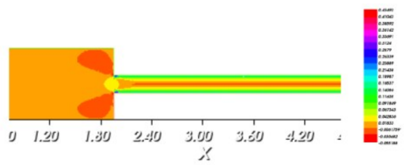

Fig. 32: The component of σ_{11} (partial view) with $Re = 100$and $We = 1$.

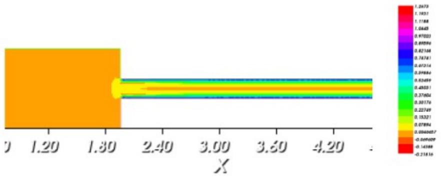

Fig. 33: The component of σ_{11} (partial view) with $Re = 100$and $We = 4.6$.

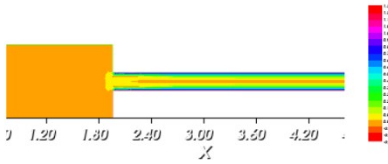

Fig. 34: The component of σ_{11} (partial view) with $Re = 100$and $We = 5.03$.

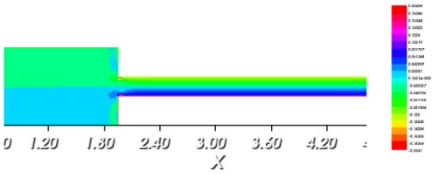

Fig. 35: The component of σ_{12} (partial view) with $Re = 100$and $We = 1$.

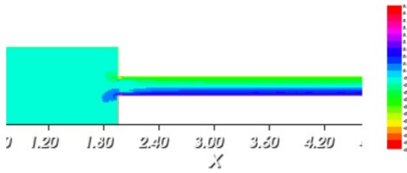

Fig. 36: The component of σ_{12} (partial view) with $Re = 100$and $We = 4.6$.

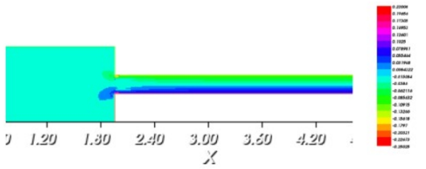

Fig. 37: The component of $\sigma_{12}$with $Re = 100 We = 5.03$.

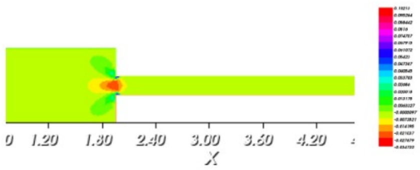

Fig. 38: The component of σ_{22} with $Re = 100$and $We = 1$.

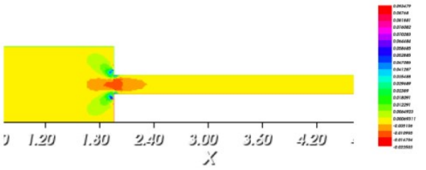

Fig. 39: The component of σ_{22} (partial view) with $Re = 100$and $We = 4.6$.

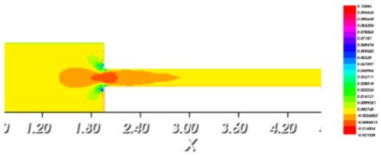

Fig. 40: The component of σ_{22} (partial view) with $Re = 100$and $We = 5.03$.

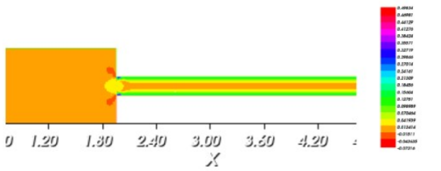

Fig. 41: The component of σ_{11} (partial view) with $Re = 500$and $We = 1$.

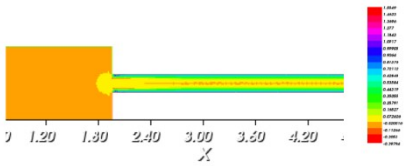

Fig. 42: The component of σ_{11} (partial view) with $Re = 500$and $We = 4.6$.

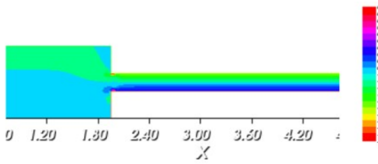

Fig. 43: The component of σ_{12} (partial view) with $Re = 500$ and $We = 1$.

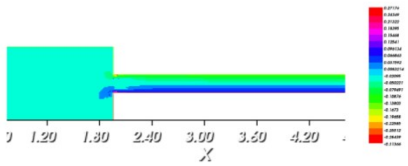

Fig. 44: The component of σ_{12} (partial view) with $Re = 500$ and $We = 4.6$.

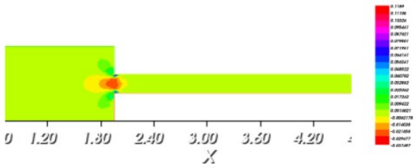

Fig. 45: The component of σ_{22} (partial view) with $Re = 500$and $We = 1$.

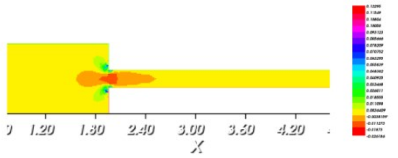

Fig. 46: The component of σ_{22} (partial view) with $Re = 500$and $We = 4.6$.

V. Conclusions

The two-dimensional steady flow of an Oldroyd-B fluid over a four-to-one abrupt contraction was investigated. This mixed problem of elliptic-hyperbolic type was decoupled into two auxiliary problems, namely, the Navier-Stokes system and the tensorial transport problem. The approach and discrete problem of Oldroyd-B model were discussed. Numerical results have been obtained in a four-to-one planar contraction (abrupt contraction) for different values of Weissenberg numbers We and Reynolds numbers Re.We observed the viscoelastic behaviors of the fluids by comparing the results from the plot of the velocity, pressure and tensor for different values of Re and We. For Newtonian flows, both the quantitative and qualitative behaviors of the kinematics were found almost same.But the differences of the types of recirculation, and their zones for the viscoelastic flows have been observed in relation to the Newtonian fluids flows through the stream function. In case of viscoelastic flows, the convergence of the algorithm is influenced by the values of Reynolds and Weissenberg. The two re-entrant corners were the reasons for which the problem fails to converge if we consider the high value of Weissenberg number. The big differences of the behaviors of the components of tensors σ_{11} and σ_{22}were also observed. For these components, the influence of $We$was notable. For a fixed value of Reynolds number, we found a limit for maximum Weissenberg number for which the applied method diverges.

References

I. A. Ern and J. Guermond, "Discontinuous Galerkin Methods for Friedrichs' Systems, I. General Theory", SIAM J. Numer. Anal., Vol. 44, Issue: 2,pp. 753-778, 2006.

II. A. Quarteroni and A. Valli, Numerical Approximation of Partial Differential Equations. Springer-Verlag 1994.

III. B. Q. Li, Discontinuous Finite Elements in Fluid Dynamics and Heat Transfer. Springer-Verlag, 2006.

IV. C. Fetecau and K. Kannan, "A note on an unsteady fow of an Oldroyd-B fluid", International Journal of Mathematics and Mathematical Sciences, Vol., 19, pp. 3185–3194, 2015.

V. F. Hecht, "New development in FreeFem++", Journal of numerical mathematics, Vol. 20, Isssue: 3-4pp. 251-266, 2012.

VI. G. F. Carey and J. T. Oden, Finite elements. Vol.VI. Fluid mechanics. The Texas Finite Element Series, VI. Prentice Hall, Inc., Englewood Cliffs, New Jersey, 1986.

VII. H. Brezis, Functional Analysis, Sobolev Spaces and Partial Differential Equations, Springer, 2011.

VIII. J. Hron, Numerical Simulation of Visco-Elastic Fluids, In: WDS' 97, Freiburg, 1997.

IX. K. M. Helal, "Numerical Solutions of Steady Tensorial Transport Equations Using Discontinuous Galerkin Method Implemented in FreeFem++", Journal of Scientific Research, Vol. 8, Issue: 1, pp.29-39, 2016.

X. K. M. Helal, "Numerical Study and CFD Simulations of Incompressible Newtonian Flow by Solving Steady Navier-Stokes Equations Using Newton's Method", Journal of Mechanics of Continua and Mathematical Sciences,Vol. 9, Issue: 2, pp. 1403-1417, 2015.

XI. K. Najib and D. Sandri, On a decoupled algorithm for solving a finite element problem for the approximation of viscoelastic fluid flow, Numer. Math.,Vol. 72, pp. 223-238, 1993.

XII. K. R. Rajagopal, On boundary conditions for fluids of differential type, A. Sequeira (ed.) Navier-Stokes Equations and Related Non-Linear Problems, Plenum Press, 273-278, 1995.

XIII. M. Jamil, C. Fetecau, and M. Imran, "Unsteady helical flows of Oldroyd-B fluids", Commun. Nonlinear. Sci. Numer. Simulat.,Vol. 16, pp.1378–1386, 2011.

XIV. M. M. Rhaman and K. M. Helal, "Numerical Simulations of Unsteady Navier-Stokes Equations for incompressible Newtonian Fluids using FreeFem++ based on Finite Element Method", Annals of Pure and Applied Mathematics, Vol.6, Issue: 1, pp. 70-84, 2014.

XV. M. Sulaiman, A. Ali and S. Islam, "Heat and Mass Transfer in Three-Dimensional Flow of an Oldroyd-B Nanofluid with Gyrotactic Micro-Organisms", Mathematical Problems in Engineering, Vol. 2018, ID 6790420.

XVI. M. Jamil, C. Fetecau, and M. Imran, "Unsteady helical flows of Oldroyd-B fluids", Commun. Nonlinear. Sci. Numer. Simulat.,Vol. 16, pp.1378–1386, 2011.

XVII. M. Pires, A. Sequeira, "Flows of Generalized Oldroyd-B Fluids in Curved Pipes", In: Escher J. et al. (eds) Parabolic Problems. Progress in Nonlinear Differential Equations and Their Applications, vol 80. Springer, Basel, 2011.

XVIII. M. M. Rhaman and K. M. Helal, "Numerical Simulations of Unsteady Navier-Stokes Equations for incompressible Newtonian Fluids using Free Fem++ based on Finite Element Method", Annals of Pure and Applied Mathematics**,** Vol.6, Issue: 1, pp. 70-84, 2014.

XIX. M. Sulaiman, A. Ali and S. Islam, "Heat and Mass Transfer in Three-Dimensional Flow of an Oldroyd-B Nanofluid with Gyrotactic Micro-Organisms", Mathematical Problems in Engineering*,* Vol. 2018, ID 6790420.

XX. Oldroyd, James, "On the Formulation of Rheological Equations of State", Proceedings of the Royal Society of London. Series A, Mathematical and Physical Sciences, Vol. 200, Issue: 1063,pp. 523–541, 1950

XXI. P. Lesaint and P. A. Raviart, On a finite element method for solving the neutron transport equation, C. Boor (editor), Mathematical Aspects of Finite Elements in Partial Differential Equations, 89-123, New York, Academic press, 1974.

XXII. P. Saramito, Simulation numeerique decoulements de fluids visco-elastiquespar elements finis incompressible setune methode de directions alternes Applications, These de l'Institut National Polytechnique de Grenoble, 1990.

XXIII. S. A. Shehzad, A. Alsaedi, T. Hayat, and M. S. Alhuthali, "Three-Dimensional Flow of an Oldroyd-B Fluid with Variable Thermal Conductivity and Heat Generation/Absorption", PLoSONE,Vol. 8, 2013.

XXIV. T. Hayat and A. Alsaedi, "On thermal radiation and Joule heating effects on MHD flow of an Oldroyd-B fluid with thermophoresis", Arb. J. Sci. Eng.,Vol. 36, pp.1113–1124, 2011.

XXV. T. Hayat, S. A. Shehzad, M. Mustafa, and A. A. Hendi, "MHD flow of an Oldroyd-B fluid through a porous channel", Int. J. Chem. Reactor Eng., Vol. 10, Article ID A8, 2012.

XXVI. V. Girault and P. A. Raviart, Finite Element Approximation of the Navier-Stokes Equations, Computational Mathematics. Springer-Verlag, Berlin, 1986.